Cell Reports

Detection of Deleterious On-Target Effects after HDR-Mediated CRISPR Editing

Graphical Abstract

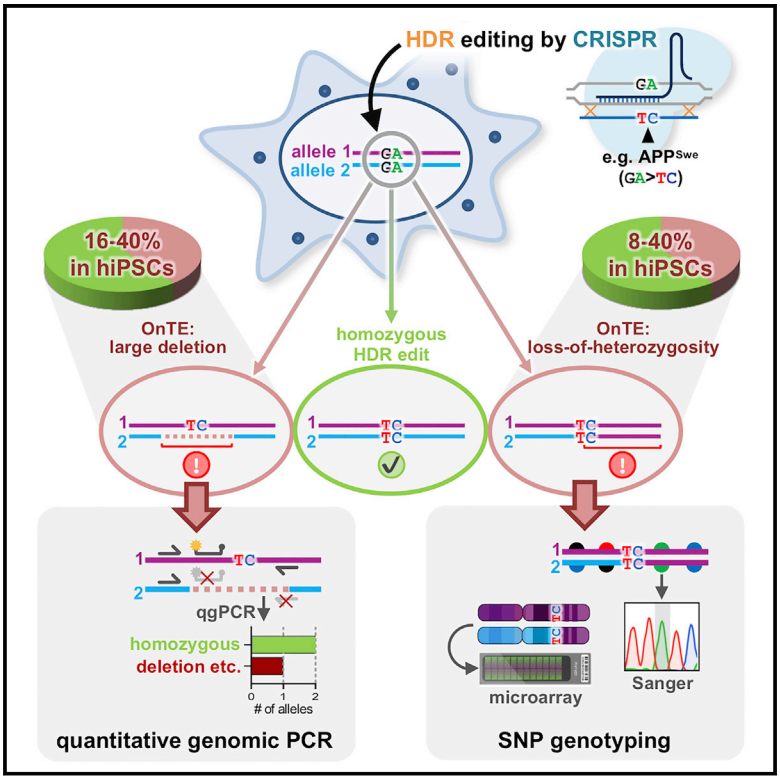

Highlights

- On-target effects (OnTEs) are present in up to 40% of human CRISPR-edited iPSC clones
- OnTEs are frequently missed by standard quality controls, such as locus sequencing
- Unnoticed OnTEs strongly affect phenotype formation in an iPSC Alzheimer model
- Simple and broadly applicable qgPCR and SNP genotyping-based tools reliably detect OnTEs

Authors

Isabel Weisheit, Joseph A. Kroeger, Rainer Malik, ..., Angelika Dannert, Martin Dichgans, Dominik Paquet

Correspondence

dominik.paquet@med.uni-muenchen.de

In Brief

Weisheit et al. show that deleterious on-target effects, such as large, mono-allelic deletions or loss of heterozygosity, are widespread in human iPSCs after CRISPR/Cas9 editing both via HDR and NHEJ. They describe simple, low-cost, and broadly applicable quantitative genomic PCR (qgPCR) and SNP genotyping-based tools to reliably identify such on-target effects.

Weisheit et al., 2020, Cell Reports *31*, 107689
May 26, 2020
https://doi.org/10.1016/j.celrep.2020.107689

Cell Reports

CellPress
OPEN ACCESS

Report

Detection of Deleterious On-Target Effects after HDR-Mediated CRISPR Editing

Isabel Weisheit,[1,2] Joseph A. Kroeger,[1,2] Rainer Malik,[1] Julien Klimmt,[1,2] Dennis Crusius,[1] Angelika Dannert,[1,2] Martin Dichgans,[1,2,3] and Dominik Paquet[1,2,3,4,*]

[1]Institute for Stroke and Dementia Research (ISD), University Hospital, LMU Munich, 81377 Munich, Germany
[2]Graduate School of Systemic Neurosciences, LMU Munich, 82152 Planegg-Martinsried, Germany
[3]Munich Cluster for Systems Neurology (SyNergy), 81377 Munich, Germany
[4]Lead Contact
*Correspondence: dominik.paquet@med.uni-muenchen.de
https://doi.org/10.1016/j.celrep.2020.107689

SUMMARY

CRISPR genome editing is a promising tool for translational research but can cause undesired editing outcomes, both on target at the edited locus and off target at other genomic loci. Here, we investigate the occurrence of deleterious on-target effects (OnTEs) in human stem cells after insertion of disease-related mutations by homology-directed repair (HDR) and gene editing using non-homologous end joining (NHEJ). We identify large, mono-allelic genomic deletions and loss-of-heterozygosity escaping standard quality controls in up to 40% of edited clones. To reliably detect such events, we describe simple, low-cost, and broadly applicable quantitative genotyping PCR (qgPCR) and single-nucleotide polymorphism (SNP) genotyping-based tools and suggest their usage as additional quality controls after editing. This will help to ensure the integrity of edited loci and increase the reliability of CRISPR editing.

INTRODUCTION

CRISPR genome editing holds great promise for biomedical research because it allows precise and efficient genomic modifications for investigations of disease-associated variants, e.g., in disease-relevant human cell types derived from induced pluripotent stem cells (iPSCs) (Hockemeyer and Jaenisch, 2016; Paquet et al., 2016). However, application of CRISPR can be hampered by unwanted off- and on-target effects (Cheng and Tsai, 2018; Thomas et al., 2019). Recent studies in mice have described frequent occurrences of large deletions and complex rearrangements at CRISPR-edited loci after repair by non-homologous end joining (NHEJ) (Adikusuma et al., 2018; Kosicki et al., 2018; Owens et al., 2019; Shin et al., 2017). It is currently unclear whether such alterations also affect clinically relevant human cells, such as iPSCs, because repair pathways involved in CRISPR editing are differentially regulated (MacRae et al., 2015), as indicated, for example, by shorter human gene conversion tracts (Paquet et al., 2016). One report identified on-target effects (OnTEs) at a single locus in an immortalized human cell line edited using stable overexpression of Cas9 and a guide RNA (gRNA) (Kosicki et al., 2018) but did not address effects of transient expression of CRISPR machinery currently used in most editing protocols. Importantly, to our knowledge, it has not been investigated whether deleterious OnTEs also occur in cells edited by homology-directed repair (HDR) to introduce specific base changes, which has high relevance in disease research and gene and cell-replacement therapies. HDR- and NHEJ-edited clones are usually identified by PCR amplification of a few hundred bases around the edited locus, followed by Sanger sequencing (Kwart et al., 2017), but such genotyping will fail to identify clones with large, mono-allelic insertions or deletions overlapping with genotyping primer-binding sites. Instead, because the alterations prevent amplification of the affected allele, such hemizygous clones will appear to be homozygously edited (Figure 1A). Even though false identification of homozygously edited clones can corrupt the reliability of entire studies, tests for such deleterious OnTEs are still lacking in most genome-editing studies. Some reports have applied primer-walk PCR (Adikusuma et al., 2018; Kosicki et al., 2018; Owens et al., 2019; Shin et al., 2017), PacBio or another deep-sequencing method (Adikusuma et al., 2018; Kosicki et al., 2018; Owens et al., 2019), or droplet digital PCR (Owens et al., 2019) to detect large on-target alterations, but these methods are expensive, laborious, or require specific expertise and equipment. Here, we investigated whether large, mono-allelic deletions or insertions occur in human iPSCs after HDR-mediated CRISPR genome editing and developed quantitative genotyping PCR (qgPCR) as a simple and broadly applicable tool for their reliable detection. Strikingly, we identify these OnTEs in up to 40% of iPSC clones edited via HDR with CRISPR/Cas9 at different loci and demonstrate deleterious effects on phenotype formation in an Alzheimer's disease iPSC line. Extending on an earlier study (Ikeda et al., 2018), we also describe large regions of copy-neutral loss-of-heterozygosity (LOH) upon HDR-mediated editing in 8%–40% of clones and validate Sanger sequencing and microarray-based tools for LOH detection. Lastly, we investigated occurrence of large on-target deletions after NHEJ-mediated CRISPR editing using qgPCR and found the loss of one allele in 50% of apparently homozygous clones.

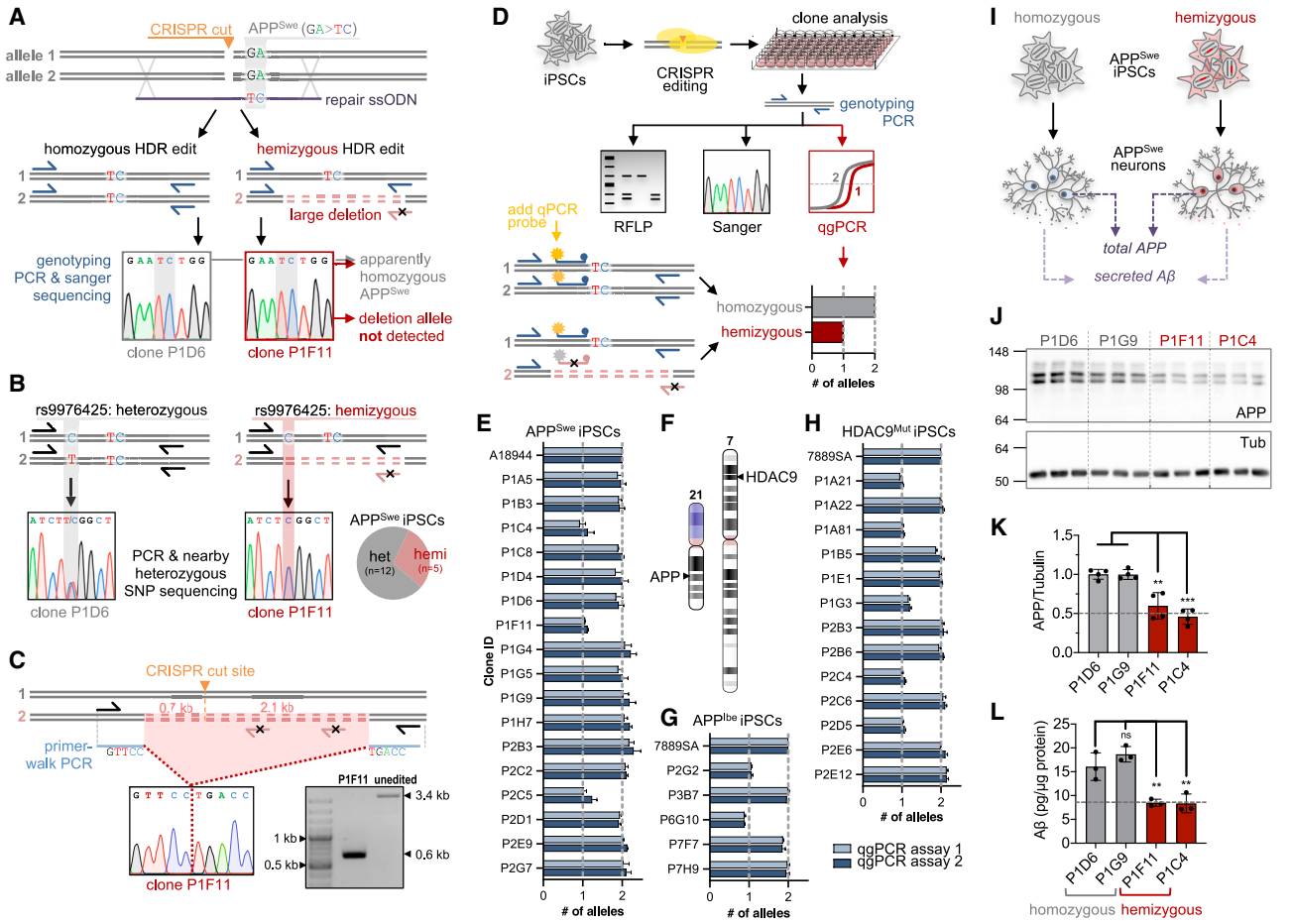

Figure 1. Deleterious OnTEs after HDR-Mediated Genome Editing in Human iPSCs

(A) Sanger genotyping fails to identify mono-allelic deletions in APP^{Swe} knockin clones.

(B) Hemizygous APP^{Swe} clones can be detected by extending genotyping PCRs to nearby heterozygous SNP rs9976425.

(C) Primer-walk PCR identified a 2.8 kb deletion in APP^{Swe} clone P1F11.

(D) Adding a qPCR probe to an existing genotyping PCR allows detection of reduced allele copy numbers by qgPCR.

(E) Allele copy numbers for two independent qgPCR assays reveal hemizygous clones with the loss of one allele after HDR knockin of APP^{Swe}. Values were normalized to the unedited parent cell line (A18944, n = 3). Data are represented as means ± SEM.

(F) Editing positions on chromosomes 21 and 7 at APP and HDAC9 loci.

(G) Identification of hemizygous clones edited at the APP^{Ibe} locus. Values were normalized to the unedited parent cell line (7889SA, n = 3). Data are represented as means ± SEM.

(H) Identification of hemizygous clones edited at the HDAC9^{Mut} locus. Values were normalized to the unedited parent cell line (7889SA, n = 3). Data are represented as means ± SEM.

(I) Two homozygous or hemizygous APP^{Swe} clones were differentiated into cortical neurons, and the levels of total APP and secreted Aβ were measured.

(J) Western blot of APP and tubulin indicates reduced APP expression in hemizygous clones.

(K) Quantification of (J) and biological replicates in Figure S2 (APP normalized to tubulin and means of homozygous clones on same gel, n = 4). Data are represented as means ± SEM. **p < 0.01, ***p < 0.001, one-way ANOVA. Dotted line indicates 50% of the means of homozygous clones.

(L) Aβ secretion (normalized to total protein amount, n = 3) is also reduced in hemizygous clones. Data are represented as means ± SEM. **p < 0.01, one-way ANOVA. Dotted line indicates 50% of the means of homozygous clones.

RESULTS

Analysis of OnTEs in HDR-Edited iPSC Clones by SNP Genotyping and PCR Primer-Walking Yields Inconsistent Results

To explore the incidence of deleterious OnTEs in CRISPR-edited iPSCs, we analyzed 17 clones with an apparently homozygous knock-in of the APP Swedish (APP^{Swe}) mutation generated using plasmid-based editing (Paquet et al., 2016; Figure 1A). APP^{Swe} causes early-onset Alzheimer's disease in patients and is used in many disease models. We reasoned that large, mono-allelic alterations could be identified by genotyping single-nucleotide polymorphisms (SNPs) near the target site that we identified to be heterozygous before editing. Large deletions or insertions in this region would prevent amplification of the aberrant allele in a PCR covering both the target and SNP site, leading to

homozygosity of the SNP in Sanger sequencing. Indeed, SNP rs9976425 appeared homozygous in five of 17 clones after editing, suggesting previously undetected mono-allelic changes (Figure 1B; Table S1). To identify possible deletions, we performed primer-walk PCRs up to 8 kb around the APP^{Swe} locus and increased the PCR extension times to detect insertions. We identified additional products in two of the five clones identified by SNP genotyping, revealing a deletion of 2.8 kb in clone P1F11 (Figure 1C) and an insertion of 4.1 kb in clone P1C4 (Figure S1; Table S1). Primer-walk PCRs were, however, not able to resolve alterations in the remaining three clones identified in the SNP assay, potentially because of PCR size limitations, illustrating the requirement for more reliable readouts. In addition, both SNP genotyping and primer-walk PCRs are not universally applicable because other loci may lack nearby heterozygous SNPs or contain regions difficult to amplify by PCR.

qgPCR Reliably Detects Widespread Occurrence of OnTEs in HDR-Edited iPSCs

An optimal assay should not only reliably identify deleterious OnTEs but also work on every edited locus, integrate well into existing gene-editing workflows, and be broadly applicable with low requirements for special knowledge and equipment. As genome-editing workflows usually contain a PCR for genotyping by RFLP and Sanger sequencing (Kwart et al., 2017), we reasoned that the simplest way of testing for mono-allelic alterations would be to determine allele copy number using the already established genotyping PCR. We addressed this by adding a labeled probe to the existing genotyping primers for quantitative genotyping PCR (qgPCR). Edited single-cell clones with large deletions or insertions will have higher cycle threshold (Ct) values, corresponding to a reduced allele copy number at the target site (Figure 1D; see design parameters in Figure S3). To test this approach, we analyzed all 17 APP^{Swe} clones by qgPCR and confirmed the results with a second, independent qgPCR assay. Compared with unedited parent cells, three clones showed copy numbers corresponding to only one allele, which all had been previously identified by SNP genotyping (Figure 1E; Table S1). Interestingly, two other clones with SNP homozygosity had normal allele numbers in both qgPCR assays, suggesting a different OnTE, such as LOH (confirmed in further analysis below). To investigate whether OnTEs occur independently of gRNA, locus, chromosome, coding region, and cell line, we repeated the analysis in a different iPSC line (7889SA; Paquet et al., 2016), edited with a different gRNA for the APP Iberian mutation (APP^{Ibe}). We also analyzed a line edited in a non-coding region near HDAC9 at rs2107595 (Figure 1F), a lead SNP identified in a recent genome-wide association study (GWAS) for stroke and coronary artery disease (Malik et al., 2018). qgPCR analysis revealed frequent loss of alleles at both loci and in both cell lines affecting two of five APP^{Ibe} and five of 13 $HDAC9^{Mut}$ clones (Figures 1G and 1H). Again, primer-walk PCRs failed to identify all affected clones. Similar to the APP^{Swe} results, SNP genotyping revealed additional clones with SNP homozygosity but normal copy number, suggesting LOH (Table S1, see further analysis below). In agreement with previous studies (Owens et al., 2019; Shin et al., 2017), large deletions were preferentially located at sites with microhomologies, suggesting involvement of the microhomology-mediated end-joining (MMEJ) pathway (Table S2). Taken together, our data show that deleterious OnTEs, such as large deletions or insertions, occur in 18%–40% of CRISPR-edited human iPSCs and that these undesired editing events can be reliably identified by simple and universal qgPCR-based assays using already optimized genotyping PCRs.

"Standard Size" qPCR Assays Fail to Reliably Detect All OnTEs

Because our qgPCR assays had amplicon sizes of around 350 bp, we also tested assays with amplicon sizes of around 150 bp, which is set as "standard" in most qPCR primer design tools. However, these were not reliable because at least one assay for each analyzed locus failed to identify all abnormal clones (P1C4 for APP^{Swe}, P2G2 for APP^{Ibe}, and P1A21 for HDAC9; see Table S1 and Figure S3 for further details). In all these cases, the edited loci appeared to have two normal alleles, even though there were insertions or deletions present. These insertions or deletions (indels) were missed because they did not directly overlap with the cut sites, and, therefore, primers for short PCRs were still able to bind and support locus amplification. Hence, locus integrity cannot be reliably tested by "standard size" qPCRs but requires our longer qgPCR design.

OnTEs Affect Phenotype Formation in an iPSC-Based Model of Alzheimer's Disease

Most of the OnTEs we found in our HDR-edited lines caused large changes on the genomic loci, which, in many cases, could result in major changes in gene expression, unless the allelic damage is compensated by the other allele. As most HDR-mediated CRISPR editing is performed to insert or correct disease-associated mutations, defective alleles may also have unintended effects on disease modeling. To investigate potential consequences of undesired OnTEs on protein expression in a disease model, we differentiated APP^{Swe} iPSCs with and without mono-allelic alterations into cortical neurons and measured total APP levels, as well as secretion of the APP cleavage product Aβ (Figure 1I). Hemizygous APP lines displayed a reduction in APP expression and Aβ secretion by about 50% (Figures 1J–1L and S2). Such a reduction in Aβ levels may reduce pathogenic effects or even prevent formation of Alzheimer's disease phenotypes in an affected iPSC-based disease model, thus illustrating potential negative effects of undetected OnTEs on the reliability of studies using CRISPR/Cas9 editing for disease modeling.

CRISPR/Cas9 Editing in iPSCs Can Cause LOH of Entire Chromosome Arms

Our combined SNP genotyping and qgPCR analysis revealed clones with normal allelic copy number but homozygosity at nearby SNPs at all edited loci (APP^{Swe}: P1G9 and P2E9; APP^{Ibe}: P7H9; and HDAC9: P1E1; see Figures 1E, 1G, and 1H and Table S1). We reasoned that this may result from repair of a large, mono-allelic deletion by the homologous chromosome (Figure 2A). One previous report already indicated that copy-neutral LOH can occur after HDR-mediated CRISPR editing (Ikeda et al., 2018), but it is still unclear whether that is a general phenomenon or restricted to the cell line or transgene-based editing approach

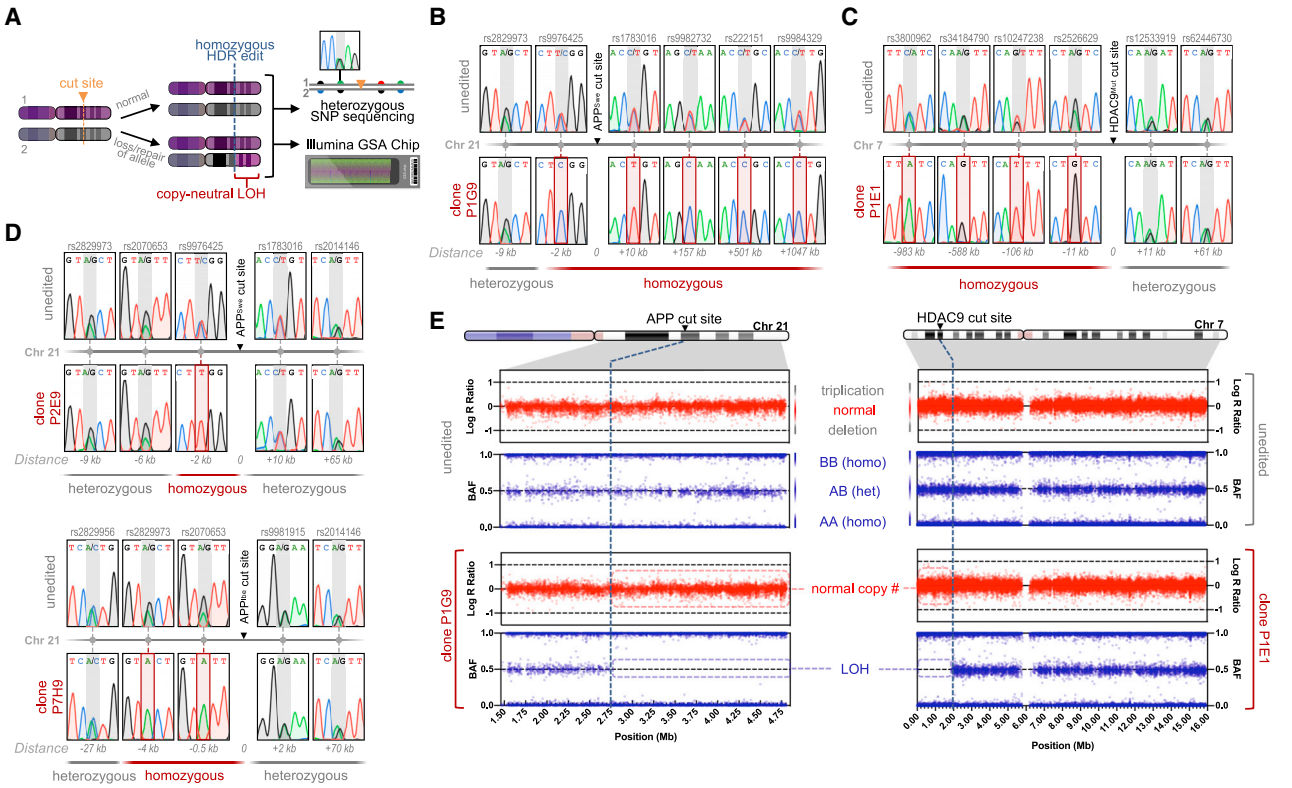

Figure 2. Detection of Copy-Neutral LOH after HDR-Mediated Genome Editing in Human iPSCs

(A) HDR editing may cause LOH, which can be detected via nearby SNP genotyping or SNP microarrays.

(B) Sanger sequencing traces of SNPs in control and edited clone P1G9 up to 1 Mb around the APP^{Swe} cut site.

(C) Sanger sequencing traces of SNPs in control and edited clone P1E1 up to 1 Mb around the HDAC9 cut site.

(D) Sanger sequencing traces of SNPs in control and edited clones around the APP^{Swe} (clone P2E9, top) or APP^{Ibe} (clone P7H9, bottom) cut sites.

(E) Log R ratio and BAF in control and edited clones for chromosome 21 (P1G9 edited for APP^{Swe}) (left) and 7 (P1E1 edited at HDAC9) (right).

described in that study. To investigate the extent of LOH in our edited iPSC lines, we identified SNPs that were heterozygous in the unedited lines on both sides of the target locus up to 1 Mb away from the cut site and analyzed their zygosity after editing. In one clone, edited at APP on chromosome 21 (P1G9), and another, edited at HDAC9 on chromosome 7 (P1E1), all tested SNPs in the direction to the end of the chromosome were homozygous (Figures 2B and 2C). Shorter regions were affected in the remaining clones (Figure 2D). To determine whether the LOH affected the entire chromosome arm in P1G9 and P1E1, we performed whole-genome SNP genotyping using the Illumina global screening array (GSA). Log R ratios showed normal copy number, but all heterozygous AB signals in B-allele frequency (BAF) were lost in the affected areas, indicating copy-neutral LOH from the cut site to the end of the targeted chromosome (Figure 2E). Taken together, our data indicate that LOH can occur after CRISPR/Cas9 editing, independent of chromosome, locus, cell line, or editing method.

OnTEs Are Also Widespread in iPSCs Edited via the NHEJ Pathway

Earlier work in mice and human cell lines indicated widespread occurrence of OnTEs after CRISPR editing via the NHEJ pathway (Adikusuma et al., 2018; Kosicki et al., 2018; Owens et al., 2019; Shin et al., 2017), but it is currently unclear whether OnTEs are also found in iPSCs, which differ in the regulation of repair pathways (MacRae et al., 2015). We, therefore, analyzed APP^{Swe} clones edited via NHEJ using the same plasmid-based CRISPR pipeline we also applied for HDR editing. We isolated clones for which loss of a restriction site overlapping the cut site indicated presence of indels and further analyzed the 28 clones in which presence of two alleles could not be shown by detection of two distinct bands in gel electrophoresis after locus PCR: 12 of these clones had differently edited alleles (i.e., double peaks in Sanger sequencing), indicating presence of two alleles, and this was confirmed by qgPCR in all cases (data not shown). Strikingly, out of the remaining 16 clones with apparently homozygous NHEJ editing (i.e., clean, single peaks in Sanger sequencing), eight had an allele copy number of only "one" in two independent qgPCR assays (Figure 3). These results were consistent with results from our nearby SNP genotyping assay: hemizygous clones identified by qgPCR were now homozygous at SNP rs9976425 (data not shown). Thus, if researchers preferentially select NHEJ clones with an apparently identical "clean" knockout on both alleles, they might have a 50% risk of using a clone with an OnTE.

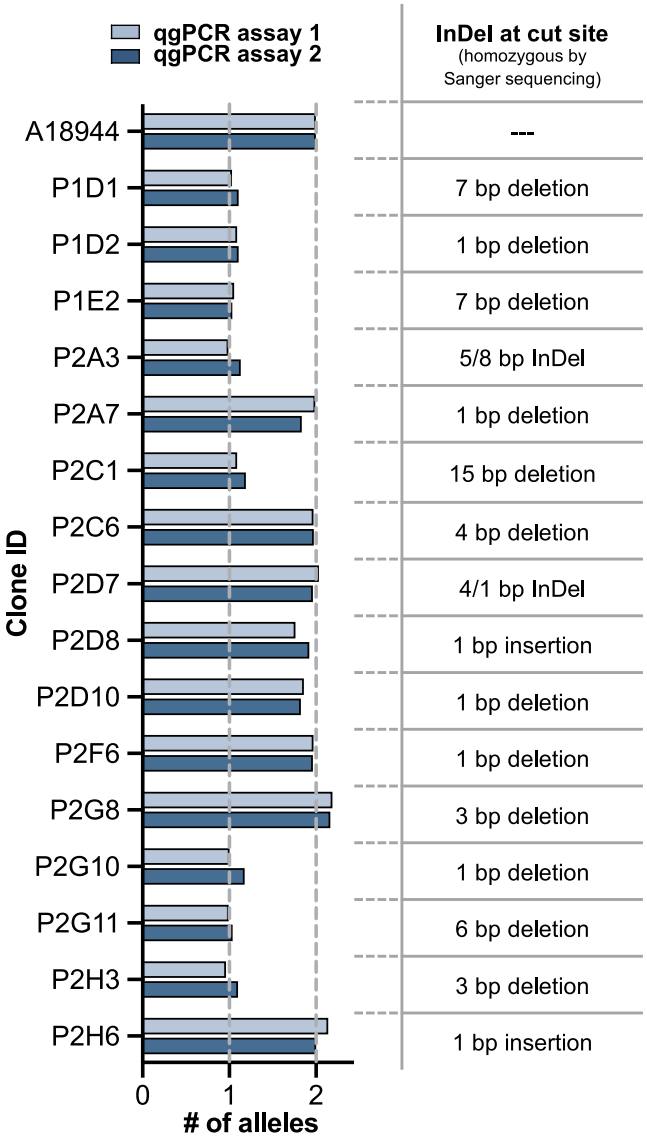

Figure 3. Widespread Formation of OnTEs after NHEJ-Mediated Genome Editing in Human iPSCs

Allele copy numbers for two independent qgPCR assays reveal hemizygous clones with the loss of one allele at the APP^{Swe} locus after NHEJ editing (left); 50% of clones with apparently homozygous editing are affected. Indel sizes as determined by Sanger sequencing (right).

DISCUSSION

The recent CRISPR revolution has provided researchers with powerful genome-editing tools that are widely applied in basic and translational research and currently also cross barriers into therapeutic applications of CRISPR-edited cells and editing directly in patients (Fellmann et al., 2017). However, CRISPR editing can cause unintended effects at the edited site and elsewhere in the genome. Although off-target effects can be efficiently detected with a variety of tools, the occurrence of OnTEs has only been described recently in mice and an immortalized human cell line. In these studies, OnTEs occurred frequently upon genome editing via the NHEJ pathway, independent of the applied CRISPR system (plasmid, RNP, and mRNA) (Adikusuma et al., 2018; Kosicki et al., 2018; Owens et al., 2019; Shin et al., 2017). However, it has been unclear whether OnTEs also occur in clinically relevant human stem cells or after editing by HDR, which is used to introduce specific base changes. We show that large, mono-allelic deletions and insertions occurred in 18%–40% of human iPSC clones after HDR-mediated CRISPR editing. These deleterious OnTEs appeared independent of the targeted locus, gRNA, coding regions, or edited cell line, suggesting widespread prevalence of on-target issues in iPSCs and also in other organisms and systems. By differentiating edited iPSCs with and without such unintended alterations into cortical neurons and comparing levels of Alzheimer's-disease-relevant Aβ secretions, we demonstrate the drastic effects unnoticed genomic alterations can have on studies using CRISPR-edited cells. Confirming and extending on earlier work in other systems, we also demonstrate the presence of OnTEs in up to 50% of iPSCs edited via the NHEJ pathway.

Furthermore, we also observed the occurrence of copy-neutral LOH after CRISPR editing, affecting entire chromosome arms. Similar LOH has also been described in human pre-implantation embryos edited by CRISPR to correct heterozygous mutations by interhomolog recombination (Ma et al., 2017). However, a major difference to our study is that the LOH allele did not simply acquire the sequence of the other allele but, in addition, contained the mutation introduced by the repair template used for HDR. This difference indicates a more complex repair scenario, in which it is not obvious that one allele acquired the sequence of the other. Such loss of SNP heterozygosity may potentially alter gene expression or expose effects of recessive mutations, which could be detrimental, especially in edited human embryos and clinical applications of iPSCs. Our findings highlight the need for technologies that reliably detect all unwanted OnTEs. Standard quality controls broadly performed in the field, such as genotyping or karyotyping, will only detect small events restricted to genotyping amplicons or very large chromosomal aberrations, such as megabase-sized deletions, translocations, and inversions, but miss the CRISPR-induced OnTEs that we and others have revealed (Adikusuma et al., 2018; Ikeda et al., 2018; O'Keefe et al., 2010; Owens et al., 2019; Shin et al., 2017).

Moreover, high-density SNP arrays sometimes used for quality controls faithfully detect only larger deletions, inversions, and LOH because their reliability increases with the number of affected SNPs. LOH affecting single SNPs may be visible, but the reliability of chip data for single SNPs is less than it is for Sanger sequencing and often depends on the detection probe, genomic location, etc. Copy-neutral inversions are usually invisible in chip assays. Many of the OnTEs that we found were small, affecting only a couple hundred to a few thousand base pairs. Accordingly, these events overlapped with no, a single, or only a few SNPs. Although such small events could be reliably detected by qgPCR (deletions, insertions, and inversions) or our Sanger sequencing-based assay (LOH), they could not be faithfully detected by the standard GWAS chip technology we used. Using higher-density chips would not solve that problem

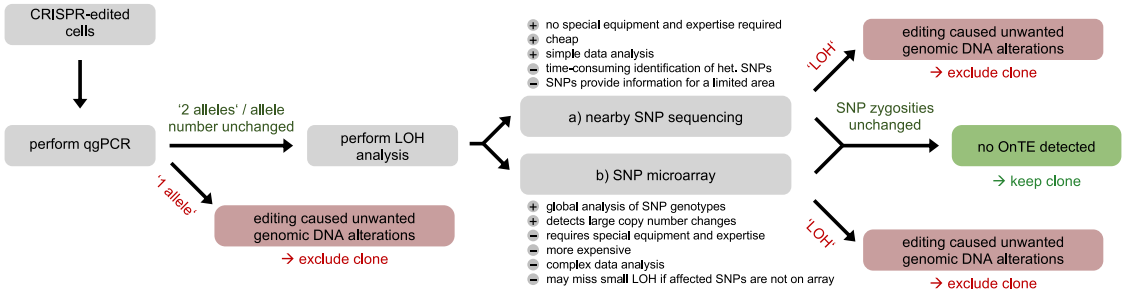

Figure 4. Workflow of Suggested Quality Control Experiments to Determine OnTEs after CRISPR Editing

Single-cell clones edited by CRISPR/Cas9 are first subjected to analysis by qgPCR to confirm unchanged allele numbers in edited clones and to exclude clones with altered allelic copy number. To check clones for loss of heterozygosity (LOH), there are two possibilities: nearby SNP sequencing and SNP microarrays. Both methods have their individual advantages, and the selection needs to be made according to the researchers' needs: Nearby SNP sequencing is cheap and does not require special equipment or expertise for analysis, whereas SNP microarrays are more expensive and involve complex data analysis. Local SNP sequencing is more sensitive toward small regions of LOH that overlap with only a few SNPs, but identifying those heterozygous SNPs on both sides of the target site can be laborious in contrast to a fast analysis by microarrays. Furthermore, SNP microarrays analyze SNP genotypes genome-wide and enable characterizing the dimension of large regions of LOH, whereas nearby SNP genotyping is restricted to a few loci around the edited site. Taken together, a combination of qgPCR analysis, and nearby SNP genotyping, and/or clone analysis by SNP microarrays should be conducted after CRISPR/Cas9 genome editing to ensure the integrity of the edited loci.

because the detection is not limited by the overall number of measured SNPs on the chip but by the number of measurable affected SNPs around the edited locus. We, therefore, developed and validated assays based on qgPCR, Sanger sequencing, and microarrays, which in combination allow reliable detection of OnTEs in iPSCs and other systems. We selected these techniques because of their simplicity, low cost, easy integration into existing workflows, universal applicability for HDR- and NHEJ-mediated CRISPR editing in various systems, and feasibility for non-specialist laboratories to allow broad dissemination and acceptance in the field. We suggest using both qgPCR and nearby or global SNP genotyping as additional quality-control measures to increase the reliability of CRISPR editing (see detailed workflow in Figure 4) in iPSCs and other systems.

In this study, we focused on developing reliable assays for OnTE detection to meet the urgent need of the CRISPR field for thorough quality-control measures of edited cells and animals. However, future work should be aimed at not only detecting these OnTEs but also understanding their biological roots and reasons for occurrence, leading to strategies to avoid their formation in the first place. This could be addressed by studying (1) the locus-dependent influences, such as chromatin structure; (2) the effects of genome-editing reagents, e.g., by using Cas9 nickase or another nuclease; (3) the effects of repair templates by modulating the single-stranded oligodeoxynucleotides (ssODN) design and orientation; and (4) the influences of other repair pathways, e.g., by modulating the NHEJ or MMEJ pathways using knockdowns or specific inhibitors.

STAR★METHODS

Detailed methods are provided in the online version of this paper and include the following:

- KEY RESOURCE TABLE
- RESOURCE AVAILABILITY
  - Lead Contact
  - Materials Availability
  - Data and Code Availability
- EXPERIMENTAL MODEL AND SUBJECT DETAILS
  - iPSC lines
  - CRISPR/Cas9 genome editing
  - iPSC culture, electroporation and cortical differentiation
- METHOD DETAILS
  - Genotyping assay design and copy number analysis by quantitative genotyping PCR (qgPCR)
  - GSA Illumina Chip
  - Genomic variant identification
  - Primer-walk PCR
  - Measurements of total APP and Amyloid-β
- QUANTIFICATION AND STATISTICAL ANALYSIS

SUPPLEMENTAL INFORMATION

Supplemental Information can be found online at https://doi.org/10.1016/j.celrep.2020.107689.

ACKNOWLEDGMENTS

This work was supported by grants from the Deutsche Forschungsgemeinschaft (DFG, German Research Foundation) under Germany's Excellence Strategy within the framework of the Munich Cluster for Systems Neurology (EXC 2145 SyNergy; grant no. 390857198), Vascular Dementia Research Foundation, VERUM Foundation, Wilhelm-Vaillant-Foundation, and the donors of the ADR AD2019604S, a program of the BrightFocus Foundation (to D.P.). We thank Peter Lichtner for GSA chip analysis, Johannes Trambauer and Harald Steiner for help with the APP western blots, Brigitte Nuscher for help with the Aβ MSD, and Benedikt Wefers for helpful comments.

AUTHOR CONTRIBUTIONS

Conceptualization, I.W. and D.P.; Methodology, I.W., J.A.K., R.M., and D.P.; Investigation, I.W., J.A.K., R.M., J.K., D.C., and A.D.; Writing – Original Draft,

I.W., J.A.K., R.M., and D.P.; Writing – Review & Editing, I.W., J.A.K., R.M., J.K., A.D., M.D., and D.P.; Funding Acquisition, M.D. and D.P.; Supervision, M.D. and D.P.

DECLARATION OF INTERESTS

The authors declare no competing interests.

Received: November 27, 2019
Revised: April 22, 2020
Accepted: May 4, 2020
Published: May 26, 2020

REFERENCES

Adikusuma, F., Piltz, S., Corbett, M.A., Turvey, M., McColl, S.R., Helbig, K.J., Beard, M.R., Hughes, J., Pomerantz, R.T., and Thomas, P.Q. (2018). Large deletions induced by Cas9 cleavage. Nature *560*, E8–E9.

Cheng, Y., and Tsai, S.Q. (2018). Illuminating the genome-wide activity of genome editors for safe and effective therapeutics. Genome Biol. *19*, 226.

Fellmann, C., Gowen, B.G., Lin, P.-C., Doudna, J.A., and Corn, J.E. (2017). Cornerstones of CRISPR-Cas in drug discovery and therapy. Nat. Rev. Drug Discov. *16*, 89–100.

Guo, Y., He, J., Zhao, S., Wu, H., Zhong, X., Sheng, Q., Samuels, D.C., Shyr, Y., and Long, J. (2014). Illumina human exome genotyping array clustering and quality control. Nat. Protoc. *9*, 2643–2662.

Hockemeyer, D., and Jaenisch, R. (2016). Induced pluripotent stem cells meet genome editing. Cell Stem Cell *18*, 573–586.

Ikeda, K., Uchida, N., Nishimura, T., White, J., Martin, R.M., Nakauchi, H., Sebastiano, V., Weinberg, K.I., and Porteus, M.H. (2018). Efficient scarless genome editing in human pluripotent stem cells. Nat. Methods *15*, 1045–1047.

Karlsson, J.O., Ostwald, K., Kåbjörn, C., and Andersson, M. (1994). A method for protein assay in Laemmli buffer. Anal. Biochem. *219*, 144–146.

Kosicki, M., Tomberg, K., and Bradley, A. (2018). Repair of double-strand breaks induced by CRISPR-Cas9 leads to large deletions and complex rearrangements. Nat. Biotechnol. *36*, 765–771.

Kwart, D., Paquet, D., Teo, S., and Tessier-Lavigne, M. (2017). Precise and efficient scarless genome editing in stem cells using CORRECT. Nat. Protoc. *12*, 329–354.

Ma, H., Marti-Gutierrez, N., Park, S.-W., Wu, J., Lee, Y., Suzuki, K., Koski, A., Ji, D., Hayama, T., Ahmed, R., et al. (2017). Correction of a pathogenic gene mutation in human embryos. Nature *548*, 413–419.

MacRae, S.L., Croken, M.M., Calder, R.B., Aliper, A., Milholland, B., White, R.R., Zhavoronkov, A., Gladyshev, V.N., Seluanov, A., Gorbunova, V., et al. (2015). DNA repair in species with extreme lifespan differences. Aging (Albany NY) *7*, 1171–1184.

Malik, R., Chauhan, G., Traylor, M., Sargurupremraj, M., Okada, Y., Mishra, A., Rutten-Jacobs, L., Giese, A.-K., van der Laan, S.W., Gretarsdottir, S., et al.; AFGen Consortium; Cohorts for Heart and Aging Research in Genomic Epidemiology (CHARGE) Consortium; International Genomics of Blood Pressure (iGEN-BP) Consortium; INVENT Consortium; STARNET; BioBank Japan Cooperative Hospital Group; COMPASS Consortium; EPIC-CVD Consortium; EPIC-InterAct Consortium; International Stroke Genetics Consortium (ISGC); METASTROKE Consortium; Neurology Working Group of the CHARGE Consortium; NINDS Stroke Genetics Network (SiGN); UK Young Lacunar DNA Study; MEGASTROKE Consortium (2018). Multiancestry genome-wide association study of 520,000 subjects identifies 32 loci associated with stroke and stroke subtypes. Nat. Genet. *50*, 524–537.

O'Keefe, C., McDevitt, M.A., and Maciejewski, J.P. (2010). Copy neutral loss of heterozygosity: a novel chromosomal lesion in myeloid malignancies. Blood *115*, 2731–2739.

Owens, D.D.G., Caulder, A., Frontera, V., Harman, J.R., Allan, A.J., Bucakci, A., Greder, L., Codner, G.F., Hublitz, P., McHugh, P.J., et al. (2019). Microhomologies are prevalent at Cas9-induced larger deletions. Nucleic Acids Res. *47*, 7402–7417.

Paquet, D., Kwart, D., Chen, A., Sproul, A., Jacob, S., Teo, S., Olsen, K.M., Gregg, A., Noggle, S., and Tessier-Lavigne, M. (2016). Efficient introduction of specific homozygous and heterozygous mutations using CRISPR/Cas9. Nature *533*, 125–129.

Richardson, C.D., Ray, G.J., DeWitt, M.A., Curie, G.L., and Corn, J.E. (2016). Enhancing homology-directed genome editing by catalytically active and inactive CRISPR-Cas9 using asymmetric donor DNA. Nat. Biotechnol. *34*, 339–344.

Shin, H.Y., Wang, C., Lee, H.K., Yoo, K.H., Zeng, X., Kuhns, T., Yang, C.M., Mohr, T., Liu, C., and Hennighausen, L. (2017). CRISPR/Cas9 targeting events cause complex deletions and insertions at 17 sites in the mouse genome. Nat. Commun. *8*, 15464.

Steyer, B., Bu, Q., Cory, E., Jiang, K., Duong, S., Sinha, D., Steltzer, S., Gamm, D., Chang, Q., and Saha, K. (2018). Scarless genome editing of human pluripotent stem cells via transient puromycin selection. Stem Cell Reports *10*, 642–654.

Thomas, M., Burgio, G., Adams, D.J., and Iyer, V. (2019). Collateral damage and CRISPR genome editing. PLoS Genet. *15*, e1007994–e1007998.

STAR★METHODS

KEY RESOURCE TABLE

REAGENT or RESOURCE	SOURCE	IDENTIFIER
Antibodies		
APP-Y188	Abcam	ab32136; RRID:AB_2289606
Tubulin	Sigma	T5168; RRID:AB_477579
Anti-Rabbit IgG (H+L), HRP Conjugate	Promega	W4011, RRID:AB_430833
Anti-Mouse IgG (H+L), HRP Conjugate	Promega	W4021, RRID:AB_430834
Chemicals, Peptides, and Recombinant Proteins		
TfiI	NEB	R0546S
DdeI	NEB	R0175S
XmnI	NEB	R0194S
2x PrimeTime Gene Expression Master Mix	IDT	1055772
20x human TERT TaqMan Copy Number Reference Assay	ThermoFisher	4403316
OneTaq 2x Master Mix	NEB	M0486L
GeneRuler 100 bp Plus DNA ladder	ThermoFisher	SM0321
Critical Commercial Assays		
NucleoSpin Tissue Kit	Macherey-Nagel	740952
NucleoSpin Gel and PCR Clean-Up Kit	Macherey-Nagel	740609
TOPO TA Cloning Kit for Sequencing	ThermoFisher	450030
NucleoSpin Plasmid Kit	Macherey Nagel	740588
NucleoSpin RNA/Protein Kit	Macherey-Nagel	740933
MSD Human (6E10) Aβ V-PLEX Kit	Meso Scale Discovery	K15200E
Experimental Models: Cell Lines		
7889SA	Paquet et al., 2016, NYSCF	7889SA
A18944	ThermoFisher	A18945
Oligonucleotides		
sgRNAs	This paper	Table S3
ssODNs for HDR-mediated editing	This paper	Table S3
Primers	This paper	Table S3
Recombinant DNA		
MLM3636	a gift from K. Joung, Addgene	43860
pSpCas9(BB)-2A-Puro (PX459) V2.0	a gift from F. Zhang, Addgene	62988
pCas9_GFP	a gift from K. Musunuru, Addgene	44719
Software and Algorithms		
CRISPOR design tool	Tefor	http://crispor.tefor.net/
PrimerQuest design tool	IDT	N/A
PLINK	N/A	https://www.cog-genomics.org/plink/2.0/
Genome Studio 2.0	Illumina	https://emea.illumina.com/techniques/microarrays/array-data-analysis-experimental-design/genomestudio.html
Ensembl Biomart tool	Ensembl	https://www.ensembl.org/info/data/biomart/index.html
Primer3Plus	Primer3Plus	https://primer3plus.com
GraphPad Prism 8	GraphPad	N/A
Other		
Illumina Global Screening Array v2 genotyping chip	Illumina	20030770

RESOURCE AVAILABILITY

Lead Contact

Further information and requests for resources and reagents should be directed to and will be fulfilled by the Lead Contact, Dominik Paquet (dominik.paquet@med.uni-muenchen.de).

Materials Availability

All unique/stable reagents generated in this study are available from the Lead Contact with a completed Materials Transfer Agreement.

Data and Code Availability

All uncropped gels, raw qPCR data, APP and Abeta quantifications, Sanger sequencing reads and Illumina GSA chip data are available in Mendeley Data (https://dx.doi.org/10.17632/87kh5vj429.2).

EXPERIMENTAL MODEL AND SUBJECT DETAILS

iPSC lines

iPSC experiments were performed in accordance with all relevant guidelines and regulations. Work with male line 7889SA (Paquet et al., 2016) (NYSCF) was approved by the Rockefeller University Institutional Review Board after informed consent was obtained from subjects by Coriell Institute. Female iPSC line A18944 was purchased from ThermoFisher (A18945).

CRISPR/Cas9 genome editing

Single guide RNAs (sgRNAs) were designed using the CRISPR design tool (http://crispor.tefor.net/). sgRNA sequences were cloned into the BsmBI restriction site of plasmid MLM3636 (a gift from K. Joung, Addgene 43860). CRISPR editing was performed as described previously (Paquet et al., 2016) using Cas9 plasmids pSpCas9(BB)-2A-Puro (PX459) V2.0 (a gift from F. Zhang, Addgene 62988) or pCas9_GFP (a gift from K. Musunuru, Addgene 44719). Repair oligos were either symmetric 100 bp ssODNs with the same orientation as the gRNA sequence (APP^{Swe}, (Paquet et al., 2016)) or asymmetric 107 bp ssODNs (71 and 36 bp, long arm on the PAM-proximal side (Richardson et al., 2016)) with sequence complementary to the gRNA (APP^{Ibe} and HDAC9), and ordered as Ultramers from IDT.

iPSC culture, electroporation and cortical differentiation

iPSCs were maintained on Vitronectin-coated (ThermoFisher A14700) cell culture plates and grown in Essential 8 Flex Medium (ThermoFisher A2858501) at 37°C with 5% CO2. Prior to transfection, iPSCs were transferred to Geltrex-coated (ThermoFisher A1413302) cell culture plates and grown in StemFlex Medium (ThermoFisher A3349401) containing 10 μM ROCK inhibitor (Selleckchem S1049) for two days. iPS cells were transfected by electroporation as described (Kwart et al., 2017). Briefly, two million cells were resuspended in 100 μL cold BTXpress electroporation solution (VWR 732-1285) with 20 μg Cas9, 5 μg sgRNA plasmid, and 30 μg ssODN. Cells were electroporated with 2 pulses at 65 mV for 20 ms in a 1 mm cuvette (Fisher Scientific 15437270). After electroporation, cells were transferred to Geltrex-coated 10 cm plates and grown in StemFlex Medium containing 10 μM ROCK inhibitor. Cells expressing Cas9 were selected either by sorting for GFP (Kwart et al., 2017) or selection with 350 ng/ml Puromycin dihydrochloride (VWR J593) for three consecutive days starting one day after electroporation (Steyer et al., 2018). Single-cell clone colonies were picked and analyzed by RFLP assay, using NEB enzymes TfiI for APP^{Swe}, DdeI for APP^{Ibe}, XmnI for HDAC9, and Sanger sequencing as previously described (Kwart et al., 2017). Cortical neuron differentiation was performed using a dual-SMAD inhibition-based protocol as described (Paquet et al., 2016).

METHOD DETAILS

Genotyping assay design and copy number analysis by quantitative genotyping PCR (qgPCR)

Assays for qgPCR analysis of edited single-cell clones were designed using the IDT PrimerQuest design tool. Briefly, a 400-550 bp region surrounding the edited locus was entered and the amplicon size range set to 300-450 bp. The edited site was selected as excluded region for the probe to prevent overlap. If genotyping primers were available, the primer sequences were entered under partial design input. Assays in which the probe was close to the edited site were favored. For copy number analysis, genomic DNA (gDNA) was isolated with a NucleoSpin Tissue Kit (Macherey-Nagel 740952) according to manufacturer's instructions and 60 ng were used for analysis. As we occasionally observed variation in gDNA integrities from stored gDNA samples we recommend using fresh gDNA isolated at the same time from control and assayed clones. Freshly isolated gDNA was mixed with 2x PrimeTime Gene Expression Master Mix (IDT 1055772), 20x human TERT TaqMan Copy Number Reference Assay (ThermoFisher 4403316) as internal reference control, genotyping primers (0.5 pmol/μl) and the designed PrimeTime Eco Probe 5′ 6-FAM/ZEN/3′ IBFQ (0.25 pmol/μl, HPLC-purified, IDT). The qgPCR reaction was run for 2 min at 50°C, 10 min at 95°C, followed by 40 cycles of 15 s at 95°C and 1 min at 60°C. Allele copy numbers were determined by ddCt calculation relative to internal TERT reference and unedited

control; values were multiplied by two to get total number of alleles. qgPCR experiments were performed in three independent technical replicates.

GSA Illumina Chip

gDNA from all iPSC lines to be analyzed was isolated with a NucleoSpin Tissue Kit and diluted to a concentration of 75 ng/μl. Whole-genome genotyping was performed at the Helmholtz Zentrum München Genome Analysis Center (Neuherberg, Germany) using the Illumina Global Screening Array v2 genotyping chip (Illumina, San Diego, California, USA). Single nucleotide polymorphisms (SNPs) were called using the GenCall algorithm. All samples analyzed showed a sample call rate > 0.99. Gender checks were performed as an additional quality control step using PLINK2 (https://www.cog-genomics.org/plink/2.0/). SNPs with a call rate < 0.9 were discarded. All SNPs were filtered using a Hardy-Weinberg equilibrium p-value cutoff of 1E-4 and a GenTrain score cutoff of 0.7 to ensure correct clustering (Guo et al., 2014). Log R Ratio and B Allele Frequency were extracted using Genome Studio 2.0 (Illumina, San Diego, California, USA).

Genomic variant identification

Potential genomic variants within 5 kb around the edited loci were identified using the Ensembl Biomart tool (http://www.ensembl.org//useast.ensembl.org/info/data/biomart/index.html?redirectsrc=//www.ensembl.org%2Finfo%2Fdata%2Fbiomart%2Findex.html) with the following settings and filters: Ensembl variation 98 database, human Short Variants (SNPs and InDels excluding flagged variants), respective chromosome with a region of around 5kb around the edited site, global minor allele frequency > = 0.2. The flanking sequence around the retrieved variants was downloaded from Ensembl and used in Primer3Plus (https://primer3plus.com/) to design primers for SNP genotyping. Prior to Sanger sequencing, the amplicons were analyzed for size differences by agarose gel electrophoresis to check for length polymorphisms. Heterozygosity of SNPs was confirmed by identification of double peaks in Sanger sequencing in unedited versus edited iPSC. Heterozygous SNPs in a 1 Mb region around the edited loci were identified by parsing data from a previous molecular karyotyping experiment performed in unedited parent lines using the Illumina bead array HumanOmni2.5Exome-8 BeadChip v1.3 (Life & Brain GmbH, Bonn) (data not shown).

Primer-walk PCR

Primer-walk PCRs were performed with edited single-cell clones to identify aberrant PCR products with OneTaq 2x Master Mix (NEB M0486L) following manufacturer's instructions. Primers with increasing distance to the cut site in steps of around 500 bp were tested. PCR products were analyzed by agarose gel electrophoresis with a GeneRuler 100 bp Plus DNA ladder (ThermoFisher SM0321). If additional bands, not present in the unedited control cell line, were detected, PCR products were gel-purified using a NucleoSpin Gel and PCR Clean-Up Kit (Macherey-Nagel 740609) followed by Sanger sequencing. If sequencing was not successful, PCR products were TOPO cloned following manufacturer's instructions (TOPO TA Cloning Kit for Sequencing, ThermoFisher 450030). Plasmids with TOPO-cloned inserts were isolated using the NucleoSpin Plasmid kit (Macherey Nagel 740588) and Sanger sequenced.

Measurements of total APP and Amyloid-β

Total protein was extracted from differentiated neurons at DIV 35 with the NucleoSpin RNA/Protein Kit (Macherey-Nagel 740933) according to manufacturer's instructions, separated on 8% TRIS-Glycine hand-casted gels, transferred to nitrocellulose membranes (Amersham Protran 0.45 NC, GE Healthcare), boiled for 5 min in PBS, and blocked for 1 h using 0,2% I-Block (ThermoFisher T2015) with 0,1% Tween20 (Merck) in PBS. Primary antibodies (APP-Y188, Abcam ab32136, 1:4,000; Tubulin, Sigma T5168, 1:4000) were diluted in blocking solution and incubated with the membrane overnight at 4°C. After three washes in PBS + 1% Tween20, HRP-labeled secondary antibodies (Anti-Rabbit IgG (H+L), HRP Conjugate, Promega, W4011; Anti-Mouse IgG (H+L), HRP Conjugate, Promega, W4021) were added for 1h and protein signals were detected using Pierce ECL Western Blotting Substrate kit (ThermoFisher 32109), using a Fujifilm LAS4000 luminescence imager and band intensities quantified using ImageJ. For Aβ measurements, cell supernatant was conditioned for 5 days and experiments were performed in 3 biological replicates. Supernatants from experiments collected at different time points were flash-frozen in liquid nitrogen and stored at −80°C. Secreted Aβ1−38, Aβ1−40 and Aβ1−42 were measured with MSD Human (6E10) Aβ V-PLEX kits (Meso Scale Discovery) according to the manufacturer's directions. Aβ values were combined to obtain total Aβ and normalized to total protein levels from cell lysate determined by the Karlsson et al. (1994) method, as described in the NucleoSpin RNA/Protein Kit.

QUANTIFICATION AND STATISTICAL ANALYSIS

No statistical methods were used to predetermine sample size and the experiments were not randomized. Experimental data was analyzed for significance using GraphPad Prism 8. Multiplicity-adjusted $p < 0.05$ was considered statistically significant. Significance was analyzed by one-way ANOVA comparing the mean of each column with the mean of the control followed by multiple-comparison post-testing with Dunnett's method. The analysis approaches have been justified as appropriate by previous biological studies, and all data met the criteria of the tests. The investigators were not blinded to allocation during experiments and outcome assessment.

Cell Reports, Volume *31*

Supplemental Information

Detection of Deleterious On-Target Effects after HDR-Mediated CRISPR Editing

Isabel Weisheit, Joseph A. Kroeger, Rainer Malik, Julien Klimmt, Dennis Crusius, Angelika Dannert, Martin Dichgans, and Dominik Paquet

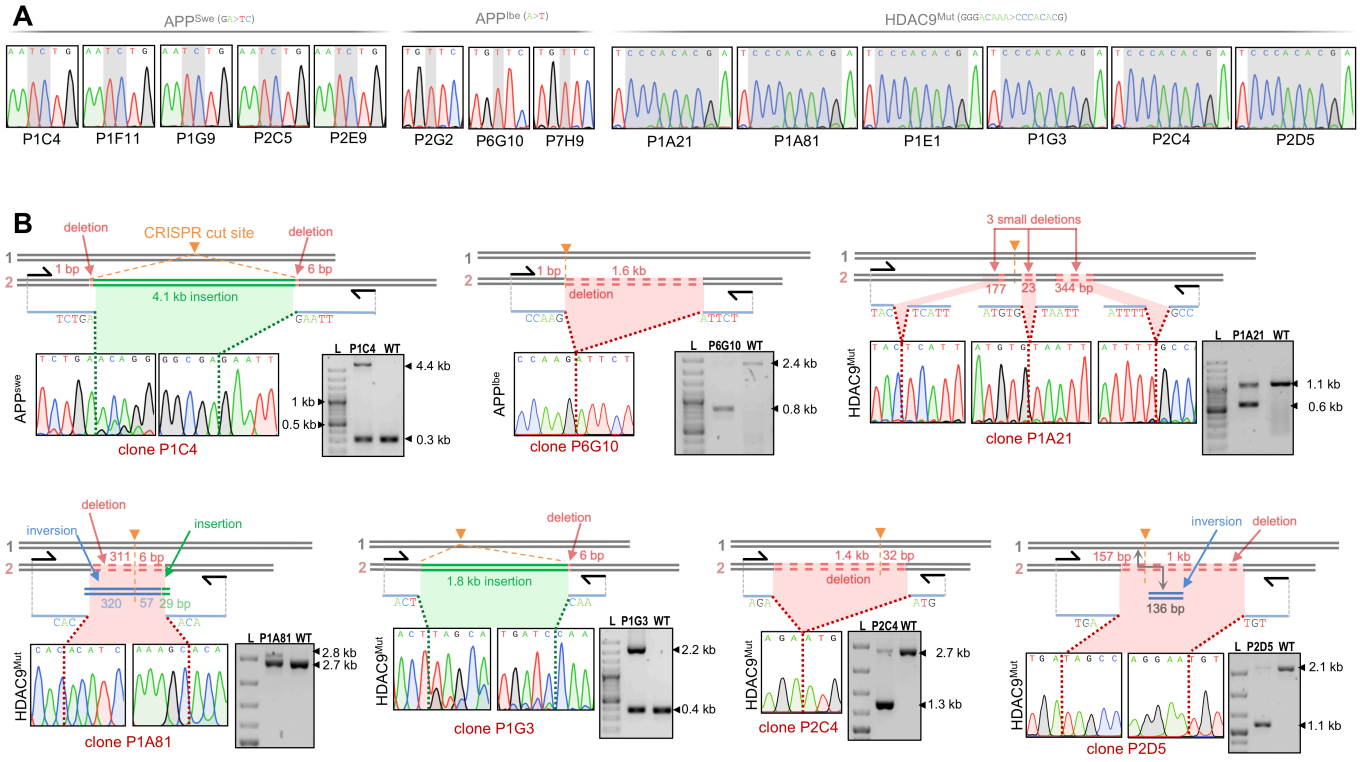

Figure S1. Genotyping results and primer-walk PCRs in CRISPR-edited clones, related to Figure 1.
(**A**) Sanger genotyping suggests homozygous HDR editing of APP^{Swe}, APP^{Ibe} and HDAC9^{Mut} in single-cell clones later identified to have mono-allelic deletions, insertions or LOH (see also Supplementary Table 1).
(**B**) Primer-walk PCR identified alleles with insertions, deletions or inversions for APP^{Swe} (top left), APP^{Ibe} (top middle), and HDAC9^{Mut} clones (remaining 5 clones). L: DNA ladder, WT: wildtype. The wildtype allele is hardly visible in some clones, potentially due to preferential amplification of the shorter PCR product.

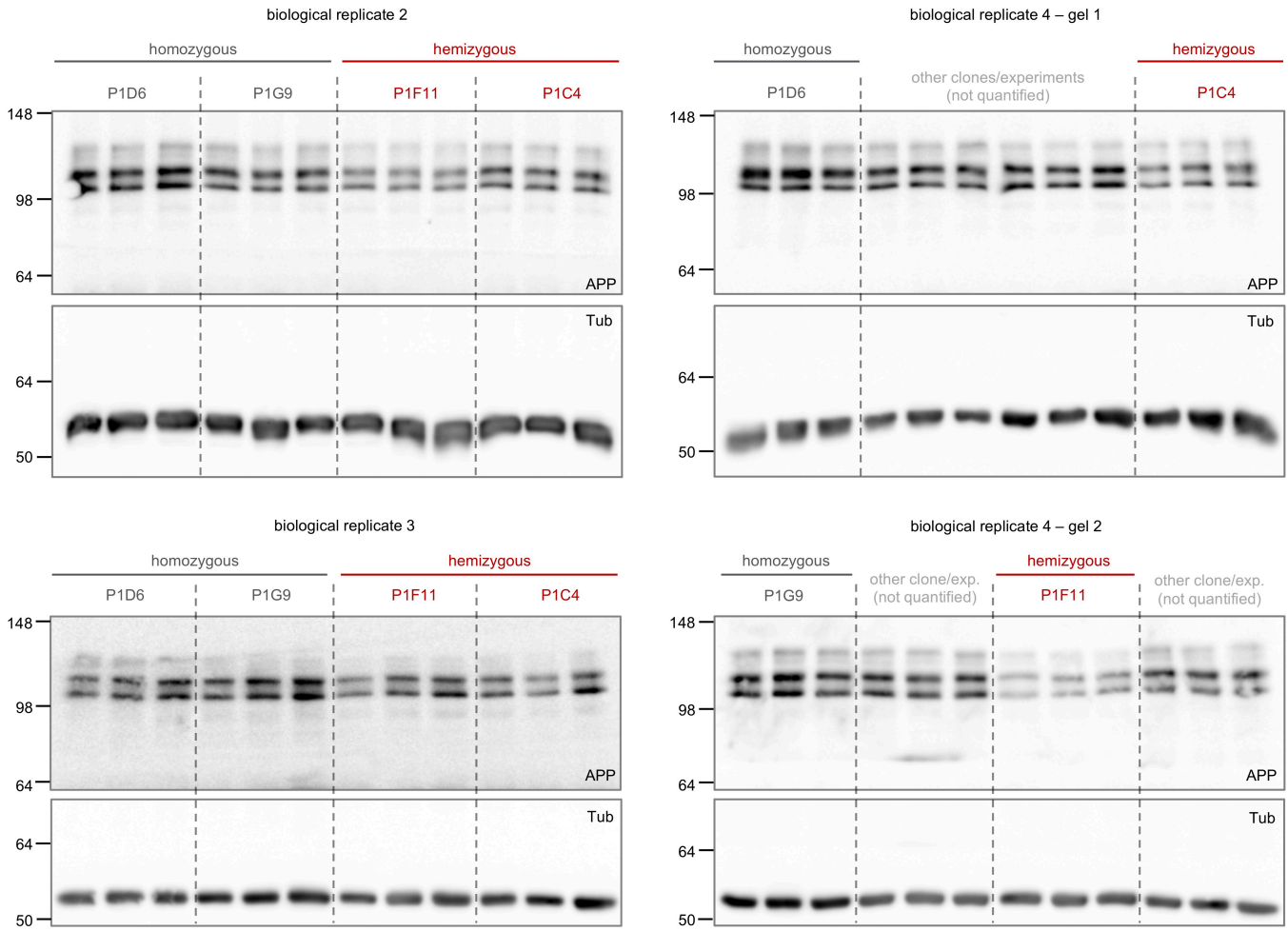

Figure S2. Quantification of APP expression in CRISPR-edited clones, related to Figure 1.
Western blot images of biological replicates 2-4 with APP and β-Tubulin expression used for quantification shown in Figure 1K. Loading controls (β-Tubulin) were run on the same blot as APP and quantitative comparisons were only performed between samples on the same blot.

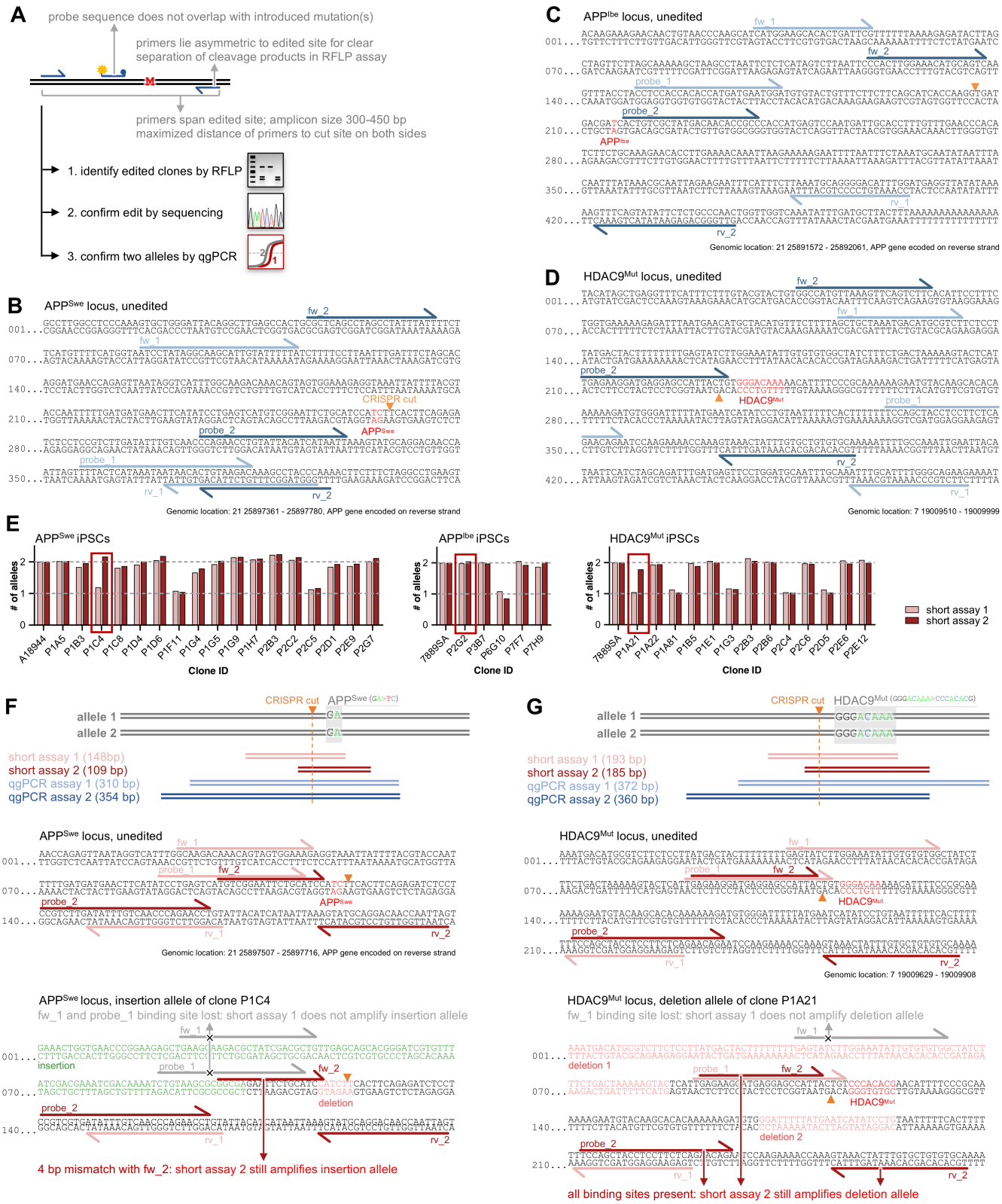
A
probe sequence does not overlap with introduced mutation(s)
primers lie asymmetric to edited site for clear separation of cleavage products in RFLP assay
M
primers span edited site; amplicon size 300-450 bp
maximized distance of primers to cut site on both sides
1. identify edited clones by RFLP
2. confirm edit by sequencing
3. confirm two alleles by qgPCR
B
APPSwe locus, unedited
fw_2
fw_1
CRISPR cut
APPSwe
probe_2
probe_1
rv_1
rv_2
Genomic location: 21 25897361 - 25897780, APP gene encoded on reverse strand
C
APPIbe locus, unedited
fw_1
fw_2
probe_1
probe_2
APPIbe
rv_1
rv_2
Genomic location: 21 25891572 - 25892061, APP gene ecoded on reverse strand
D
HDAC9Mut locus, unedited
fw_2
fw_1
probe_2
HDAC9Mut
probe_1
rv_2
rv_1
Genomic location: 7 19009510 - 19009999
E
APPSwe iPSCs
APPIbe iPSCs
HDAC9Mut iPSCs
# of alleles
A18944 P1A5 P1B3 P1C4 P1C8 P1D4 P1D6 P1F11 P1G4 P1G5 P1G9 P1H7 P2B3 P2C2 P2C5 P2D1 P2E9 P2G7
7889SA P2G2 P3B7 P6G10 P7F7 P7H9
7889SA P1A21 P1A22 P1A81 P1B5 P1E1 P1G3 P2B3 P2B6 P2C4 P2C6 P2D5 P2E6 P2E12
Clone ID
short assay 1
short assay 2
F
CRISPR cut
APPSwe (GA>TC)
allele 1
allele 2
short assay 1 (148bp)
short assay 2 (109 bp)
qgPCR assay 1 (310 bp)
qgPCR assay 2 (354 bp)
APPSwe locus, unedited
fw_1
fw_2
probe_1
probe_2
APPSwe
rv_1
rv_2
Genomic location: 21 25897507 - 25897716, APP gene encoded on reverse strand
APPSwe locus, insertion allele of clone P1C4
fw_1 and probe_1 binding site lost: short assay 1 does not amplify insertion allele
insertion
deletion
4 bp mismatch with fw_2: short assay 2 still amplifies insertion allele
G
CRISPR cut
HDAC9Mut (GGGACAAA>CCCACACG)
allele 1
allele 2
short assay 1 (193 bp)
short assay 2 (185 bp)
qgPCR assay 1 (372 bp)
qgPCR assay 2 (360 bp)
HDAC9Mut locus, unedited
Genomic location: 7 19009629 - 19009908
HDAC9Mut locus, deletion allele of clone P1A21
fw_1 binding site lost: short assay 1 does not amplify deletion allele
deletion 1
deletion 2
all binding sites present: short assay 2 still amplifies deletion allele

Figure S3. Design of quantitative PCR assays for detection of allele copy numbers in CRISPR-edited iPSCs, related to Figures 1 and 3. (**A**) Design parameters and guidelines for qgPCR assays around inserted mutation(s) 'M'. By using the same "base PCR" as for RFLP and Sanger sequencing, qgPCR assays on edited single-cell clones easily integrate into existing genome editing workflows.
(**B-D**) Positions of two independent qgPCR assays around APP^{Swe} (**B**), APP^{Ibe} (**C**) and $HDAC9^{Mut}$ (**D**) loci shown in Figure 1, with forward primer (fw), reverse primer (rv) and qPCR probe (Full primer names, as listed in Methods: APP_Swe_Gt…, APP_Ibe_Gt…, HDAC9_Gt_...).
(**E**) 'Standard' short amplicon qPCR assays fail to detect aberrant clones: Allele copy numbers for two independent short amplicon qPCR assays reveal several hemizygous clones, but at each locus one aberrant clone is not detected by either one or both short assays (red box). All values normalized to unedited parent cell line (A18944 or 7889SA).
(**F**) Overview of qPCR probe designs (top), position of primers (fw, rv) and probes for short qPCR assays 1+2 at APP^{Swe} (full primer names, as listed in methods: APP_Swe_short…) (middle), and explanation of failed detection of insertion in clone P1C4 at APP^{Swe} locus (bottom).
(**G**) Overview of qPCR probe designs (top), position of primers (fw, rw) and probes for short qPCR assays 1+2 at HDAC9 (full primer names, as listed in methods: HDAC9_short…) (middle), and explanation of failed detection of insertion in clone P1A21 at $HDAC9^{Mut}$ locus (bottom).

		Copy number analysis by qPCR		LOH analysis			
Genotype by Sanger sequencing (homo-/hemizygous)	**Clone ID**	**qgPCR assay 1+2** (Figure 1E)	**Short amplicon assay 1+2** (Figure S3E)	**Zygosity at rs9976425*** (2.4 kb upstream)	**Zygosity at rs1783016**** (10 kb downstream)	**Global SNP genotyping**	**Aberrant allele**
APP^{Swe}	P1A5	2	2	heterozygous	heterozygous	not tested	-
APP^{Swe}	P1B3	2	2	heterozygous	heterozygous	not tested	-
APP^{Swe} (Figure S1A)	P1C4	**1**	**1/2 (Figure S3F)**	**homozygous**	heterozygous	no	**4.1 kb insertion, small deletions (Figure S1B)**
APP^{Swe}	P1C8	2	2	heterozygous	heterozygous	not tested	-
APP^{Swe}	P1D4	2	2	heterozygous	heterozygous	not tested	-
APP^{Swe}	P1D6	2	2	heterozygous	heterozygous	no	-
APP^{Swe} (Figure S1A)	P1F11	**1**	**1**	**homozygous (Figure 1B)**	heterozygous	no	**2.8 kb deletion (Figure 1C)**
APP^{Swe}	P1G4	2	2	heterozygous	heterozygous	not tested	-
APP^{Swe}	P1G5	2	2	heterozygous	heterozygous	not tested	-
APP^{Swe} (Figure S1A)	P1G9	2	2	**homozygous ~1 Mb LOH by further SNP genotyping analysis (Figure 2B)**	**homozygous**	**LOH until end of chromosome (Figure 2E)**	**LOH**
APP^{Swe}	P1H7	2	2	heterozygous	heterozygous	not tested	-
APP^{Swe}	P2B3	2	2	heterozygous	heterozygous	not tested	-
APP^{Swe}	P2C2	2	2	heterozygous	heterozygous	no	-
APP^{Swe} (Figure S1A)	P2C5	**1**	**1**	**homozygous**	heterozygous	no	**not resolved, potentially very large deletion**
APP^{Swe}	P2D1	2	2	heterozygous	heterozygous	not tested	-
APP^{Swe} (Figure S1A)	P2E9	2	2	**homozygous ~2 kb LOH by further SNP genotyping analysis (Figure 2D)**	**heterozygous**	no	**LOH**
APP^{Swe}	P2G7	2	2	heterozygous	heterozygous	not tested	-
Genotype by Sanger sequencing (homo-/hemizygous)	**Clone ID**	**qgPCR assay 1+2** (Figure 1G)	**Short amplicon assay 1+2** (Figure S3E)	**Zygosity at rs2070653*** (0.5 kb upstream)	**Zygosity at rs5843179*** (0.7 kb downstream)	**Global SNP genotyping**	**Aberrant allele**
APP^{Ibe} (Figure S1A)	P2G2	**1**	**2**	**homozygous**	**homozygous**	**~ 79 kb LOH**	**not resolved, potentially very large deletion and LOH**
APP^{Ibe}	P3B7	2	2	heterozygous	heterozygous	no	-
APP^{Ibe} (Figure S1A)	P6G10	**1**	**1**	**homozygous**	**homozygous**	not tested	**1.6 kb deletion (Figure S1B)**
APP^{Ibe}	P7F7	2	2	heterozygous	heterozygous	no	-
APP^{Ibe} (Figure S1A)	P7H9	2	2	**homozygous ~3 kb LOH by further SNP genotyping analysis (Figure 2D)**	**homozygous**	**~ 10 kb LOH**	**LOH**
Genotype by Sanger sequencing (homo-/hemizygous)	**Clone ID**	**qgPCR assay 1+2** (Figure 1H)	**Short amplicon assay 1+2** (Figure S3E)	**Zygosity at rs2717369*** (2 kb upstream)	**Zygosity at rs2717368*** (2 kb downstream)	**Global SNP genotyping**	**Aberrant allele**
$HDAC9^{Mut}$ (Figure S1A)	P1A21	**1**	**1/2 (Figure S3G)**	**homozygous**	**homozygous**	not tested	**3 small deletions (Figure S1B)**
$HDAC9^{Mut}$	P1A22	2	2	heterozygous	heterozygous	not tested	-
$HDAC9^{Mut}$ (Figure S1A)	P1A81	**1**	**1**	**2 PCR products of different length**	**homozygous**	no	**inversion, deletion, insertion (Figure S1B)**
$HDAC9^{Mut}$	P1B5	2	2	heterozygous	heterozygous	no	-
$HDAC9^{Mut}$ (Figure S1A)	P1E1	2	2	**homozygous ~1 Mb LOH by further SNP genotyping analysis (Figure 2C)**	**heterozygous**	**LOH until end of chromosome (Figure 2E)**	**LOH**
$HDAC9^{Mut}$ (Figure S1A)	P1G3	**1**	**1**	**homozygous**	**homozygous**	no	**1.8 kb insertion, small deletion (Figure S1B)**
$HDAC9^{Mut}$	P2B3	2	2	heterozygous	heterozygous	not tested	-
$HDAC9^{Mut}$	P2B6	2	2	heterozygous	heterozygous	not tested	-
$HDAC9^{Mut}$ (Figure S1A)	P2C4	**1**	**1**	**2 PCR products of different length**	**homozygous**	not tested	**1.4 kb deletion (Figure S1B)**
$HDAC9^{Mut}$	P2C6	2	2	heterozygous	heterozygous	not tested	-
$HDAC9^{Mut}$ (Figure S1A)	P2D5	**1**	**1**	**homozygous**	**homozygous**	not tested	**1.2 kb deletion, inversion (Figure S1B)**
$HDAC9^{Mut}$	P2E6	2	2	heterozygous	heterozygous	not tested	-
$HDAC9^{Mut}$	P2E12	2	2	heterozygous	heterozygous	no	-

* PCR for SNP genotyping was spanning the cut site
** PCR for SNP genotyping was **not** spanning the cut site

Table S1. Overview of CRISPR-edited iPSC clones at APP^{Swe}, APP^{Ibe}, $HDAC9^{Mut}$, related to Figures 1 and 2. Data of altered clones shown in indicated figures, other data not shown.

Locus	Clone ID	Retained I Deleted I Retained	Homologous bases
APP^{Swe}	P1C4	Insertion	N/A
APP^{Swe}	P1F11	AGACAGT**TCC**|GGATGTGAAT.....TCCCAAA**TCC**|TGACCTATAA	3
APP^{Ibe}	P6G10	CATCA**CCAAG**|GTGATGACGA.....GAAAG**CCAAG**|ATTCTTGTGC	5
$HDAC9^{Mut}$	P1A21 (1st Deletion)	TTCTTT**GTAC**|GTACTGTGGC.....TAAAAA**GTAC**|TCATTGAGAA	4
$HDAC9^{Mut}$	P1A21 (2nd Deletion)	AAAAGATG**TG**|GGATTTTTAT.....TCATATCC**TG**|TAATTTTTCA	2
$HDAC9^{Mut}$	P1A21 (3rd Deletion)	CAAAAATTTT|**GCCAA**ATTGA.....TAAATATTTG|**GCCAA**CTTTT	5
$HDAC9^{Mut}$	P1A81	Complex changes with duplication and inversion	N/A
$HDAC9^{Mut}$	P1G3	Insertion	N/A
$HDAC9^{Mut}$	P2C4	GGATTG**AAGA**|CATATCCCTC.....GCAAAA**AAGA**|ATGTACAAGC	4
$HDAC9^{Mut}$	P2D5	Complex changes with duplication and inversion	N/A

Table S2. Microhomologies are prevalent at large deletion sites in CRISPR-edited iPSCs, related to Figure 1. Sequences around deletion sites with microhomologies (indicated with red letters) suggesting involvement of the MMEJ pathway. Black bars indicate sites of fusion between flanking regions, intervening part is deleted.